Episodic memory in mild cognitive impairment inversely correlates with the global modularity of the cerebral blood flow network

Highlights

- The global modularity of the CBF network increases in MCI.
- Episodic memory and patient contribution to global modularity inverse correlate.
- Connectivity analysis based on SPECT confirms brain connectivity alterations in MCI.

Episodic memory in mild cognitive impairment inversely correlates with the global modularity of the cerebral blood flow network

Carlos A Sánchez Catasús[a, b, *], Antoon Willemsen[a], Ronald Boellaard[a], Luis Eduardo Juarez-Orozco[a], Juan Samper-Noa[c, d], Angel Aguila-Ruiz[b], Peter Paul De Deyn[e, f], Rudi Dierckx[a], Yasser Iturria Medina[d, g], Lester Melie-Garcia[d, h]

[a]Department of Nuclear Medicine and Molecular Imaging, University of Groningen, University Medical Center Groningen, Hanzeplein 1, 9713 GZ Groningen, the Netherlands.

[b]Center for Neurological Restoration (CIREN), Ave. 25, No. 15 805, 11 300 Playa, La Habana, Cuba.

[c]Hospital Carlos J. Finlay, Ave. 31, 11400 Playa, La Habana, Cuba.

[d]Cuban Neuroscience Center, Ave. 25, No. 15007, 11600 Playa, La Habana, Cuba.

[e]Department of Neurology and Alzheimer Research Center, University of Groningen, University Medical Center Groningen, Hanzeplein 1, 9713 GZ Groningen, the Netherlands.

[f]University of Antwerp, Institute Born-Bunge, Laboratory of Neurochemistry and Behaviour, Universiteitsplein 1, BE-2610 Antwerpen, Belgium.

[g]McConnell Brain Imaging Center, Montreal Neurological Institute, 3801 University Street, Montréal, Quebec H3A 2B4, Canada.

[h]Laboratoire de Recherche en Neuroimagerie (LREN), Centre Hospitalier Universitaire Vaudois (CHUV), Mont-Paisible 16, CH-1011 Lausanne, Switzerland.

Corresponding Author: Carlos Alfredo Sánchez-Catasús, University Medical Center Groningen, Department of Nuclear Medicine and Molecular Imaging. Hanzeplein 1, 9713 GZ Groningen, the Netherlands. Fax number: (+31) 50 – 361 16 87;

Telephone number: (+31) 50 – 361 22 05; e-mail address: c.a.sanchez.catasus@umcg.nl

Abstract

Cerebral blood flow (CBF) SPECT is an interesting methodology to study brain connectivity in mild cognitive impairment (MCI) since it is accessible worldwide and can be used as a biomarker of neuronal injury in MCI. In CBF SPECT, connectivity is grounded in group-based correlation networks. Therefore, topological metrics derived from the CBF correlation network cannot be used to support diagnosis and prognosis individually. However, methods to extract the individual patient contribution to topological metrics of group-based correlation networks were developed although not yet applied to MCI patients. Here, we investigate whether the episodic memory of 24 amnestic MCI patients correlates with individual patient contributions to topological metrics of the CBF correlation network. We first compared topological metrics of the MCI group network with the network corresponding to 26 controls. Metrics that showed significant differences were then used for the individual patient contribution analysis. We found that the global network modularity was increased while global efficiency decreased in the MCI network compared to the control. Most importantly, we found that episodic memory inversely correlates with the patient contribution to the global network modularity, which highlights the potential of this approach to develop a CBF connectivity-based biomarker at the individual level.

Keywords: Cerebral blood flow; Single-photon emission computed tomography (SPECT); Brain connectivity; Mild cognitive impairment; Episodic memory; Global network modularity.

1. Introduction

In recent years, neuroimaging studies have shown that brain connectivity is altered during the prodromal stage of mild cognitive impairment (MCI) of Alzheimer's disease (AD) (Brier et al., 2014; Buldú et al., 2011; Catricalà et al., 2015; Dai and He, 2014; Daianu et al., 2014; Jie et al., 2014; Pereira et al., 2016; Sanabria-Diaz et al., 2013; Seo et al., 2013; Son et al., 2015; Sun et al., 2014; Tijms et al., 2013; Wang et al., 2013). These findings are stimulating the study of MCI by neuroimaging analyses based on networks (Fornito and Bullmore, 2015).

Diffusion tensor imaging (DTI) and functional MRI (fMRI) are commonly used to infer brain connectivity (Brier et al., 2014; Catricalà et al., 2015; Daianu et al., 2014; Jie et al., 2014; Sun et al. 2014; Wang et al., 2013). However, these modalities are not yet part of the standard medical care. In contrast, standard structural MRI (sMRI), FDG-PET and cerebral blood flow (CBF) SPECT are frequently already part of the clinical evaluation of MCI patients. In the context of the latter modalities, connectivity is a concept grounded in group-based correlation networks, whose topology is then analyzed using graph theory (Melie-García et al., 2013; Pereira et al., 2016; Son et al., 2015; Sanabria-Diaz et al., 2013; Seo et al., 2013).

CBF SPECT is particularly interesting to study brain connectivity in MCI as it can be used as a biomarker of neuronal injury in MCI due to AD (Albert et al., 2011), equivalent to FDG-PET but less expensive and more accessible worldwide (Quaranta et al., 2018; Sánchez-Catasús et al., 2017). We previously demonstrated the feasibility of graph theoretical analysis of the CBF correlation (CBF_{corr}) network using SPECT (Melie-García et al., 2013; Sánchez-Catasús et al., 2017). Preceding reports have also shown that CBF covariance networks derived from arterial spin labeling MRI data are consistent with fMRI derived networks (Liang et al., 2012; Viviani et al., 2011). Furthermore, previous studies suggest that brain regions with higher functional connectivity need a greater CBF supply (Liang et al., 2014;

Storti et al., 2017) and a tight coupling between CBF and brain functional topology (Liang et al., 2013).

Unlike DTI and functional MRI techniques, topological network metrics derived from CBF SPECT (as FDG-PET and sMRI) are group-based, which does not allow its clinical use. Nevetherless, methods to extract individual patient information from group-based correlation networks were proposed (Batalle et al., 2013; Raj et al., 2010; Saggar et al., 2015; Tijms et al., 2012; Zhou et al., 2011), but not yet applied to MCI patients. One of these methods stands out since it is relatively easy to implement it in clinical practice (Saggar et al., 2015). This method estimates an indirect measurement of a network metric for a single patient by extracting the patient contribution to that metric. The estimation is achieved by subtracting the metric of the network using control subjects only from the metric using control subjects plus the patient. To clarify whether this approach might be clinically useful, the association between individual patient contributions to network metrics and clinical characteristics of MCI patients need to be studied. It would be particularly important to examine the relationship with the decline in episodic memory, a hallmark component and major clinical symptom in patients that progress to AD dementia (Albert et al., 2011).

In this study, we investigate whether the episodic memory of amnestic MCI patients correlates with the individual patient contributions to topological metrics of the CBF_{corr} network. Since the method for extracting the individual contribution was validated only for global metrics, we restricted the analysis to those metrics. To enable this analysis, we first compared metrics of the network corresponding to patients ºwith those of a network of cognitively healthy controls. In particular, we examined the global network modularity, since it has been shown to be more sensitive to the AD process compared to other metrics (Pereira et al., 2016). We also analyzed global and mean local efficiencies, which are typically used as metrics of network integration and segregation, respectively (Rubinov and Sporns, 2010).

2. Methods and materials

2.1. Participants

Twenty-four amnestic MCI patients and twenty-six clinically healthy control volunteers were studied, selected from one hundred subjects recruited over a two-year period and a one-year follow-up using the inclusion and exclusion criteria described below. Table 1 summarizes demographic and cognitive data in control and MCI groups. The Ethics Committee of the Center for Neurological Restoration of Havana, Cuba, approved the study. All participating subjects gave written informed consent according to the Helsinki Declaration.

All participants were screened for a complete medical history, routine blood tests, cranial MRI, and clinical, neurological/psychiatric and neuropsychological examinations. Subjects were clinically diagnosed as MCI using the criteria based on the Clinical Dementia Rating Scale (CDR). CDR is one of the clinical scales frequently used for this purpose and suited to support amnestic MCI as it is strongly weighted towards memory evaluation (Morris, 1993). Patients were classified as MCI with CDR=0.5; while normal cognitive subjects with CDR= 0. All MCI patients maintained independence in their daily living.

Inclusion criteria were: 1) patients with memory complaints as the main cognitive symptom; 2) subjects (patients and controls) with a complete neuropsychological evaluation; 3) subjects with limited (and treated) vascular risk factors, based upon clinical examination, blood tests, and magnetic resonance angiography (MRA) findings; 4) subjects without significant depression according to the Hamilton Depression Scale (score < 8) (Hamilton, 1960); 5) no prior or current treatment with acetylcholinesterase inhibitors; and 6) right-handedness.

Exclusion criteria were: 1) significant medical conditions (i.e. advanced cardiac disease, poorly controlled diabetes and hypertension, other chronic diseases); 2) cerebrovascular disorders (transient ischemic attack or cerebral infarction), moderate or severe carotid stenosis by MRA findings, large white matter changes on MRI, hydrocephalus or intracranial mass; 3)

history of traumatic brain injury or another neurological disease; 4) psychiatric disorders, substance abuse or dependence; and 5) Mini-Mental State Examination (MMSE) (Folstein et al., 1975) scores < 24.

Table 1 Demographic and cognitive data in control and MCI groups.

	Control (*n*=26)	**MCI (*n*=24)**	**p value**
Demographic data			
Age (years)	60.9 ± 7.3	65 ± 7.1	0.06 [a]
Gender (female/male)	13/13	14/10	0.58 [b]
Years of education	13.6 ± 3.9	12.6 ± 4.5	0.3 [a]
Cognitive data			
MMSE	29.3 ± 1.1	27.6 ± 1.1	10^{-6}
Rey complex fig. (delayed recall)	18.1 ± 5.2	9.9 ± 3.7	10^{-6}
Digit span (forward)	5.9 ± 1	5.7 ± 1.2	0.84
Digit span (backward)	4.9 ± 0.9	4.7 ± 0.8	0.79
Rey complex fig. (copy)	32.7 ± 4.4	31 ± 6.5	0.53
Token test	33.5 ± 2	33.4 ± 2.5	0.19
Verbal fluency	10 ± 2.9	9.5 ± 3.8	0.562
Attentive matrices	44. 9 ± 9.7	44.1 ± 9.2	0.59
Trail Making A	39.4 ± 4.7	41.9 ± 10.1	0.48
Trail Making B	107.9 ± 14.5	107.1 ± 27.8	0.741

Data shown as mean ± standard deviation. [a], Student t-tests for independent samples. [b], Chi-square test. Differences between groups for cognitive data were tested using ANCOVA, modeling group as a categorical independent variable and controlling for age, gender and years of education.

2.2. Cognitive function assessment

A neuropsychological evaluation was performed by specific tests in five cognitive domains (memory, visuospatial ability, language, attention, and the executive function) to better characterize controls and MCI patients.

The Rey Complex Figure test (RCFT), delayed recall, was used to assess non-verbal episodic memory (Lezak, 1983). A recent study showed that non-verbal episodic memory measure is a good discriminator between AD and non-AD pathologies as well as between non-semantic primary progressive aphasias (Ramanan et al., 2016).

The digit span was measured for short-term memory evaluation (Lezak, 1983). Visuospatial ability was assessed by the copy of the RCFT. Language domain was evaluated by the token test (Lezak ,1983) and a verbal fluency test (Mondini et al., 2005). The attentive matrices were used to assess attention (Spinnler and Tognoni, 1987) and trail making A and B tests for executive function evaluation (Lezak, 1983). Differences in cognitive variables between control and MCI groups were tested using ANCOVA, using group as a categorical independent variable and controlling for age, gender and years of education.

Patients that progressed to dementia at one-year follow-up by meeting the NINDS/ADRDA criteria for probable AD (McKhann et al., 1984) were identified.

2.3. SPECT imaging and construction of CBF correlation networks

CBF SPECT was carried out with a double-head rectangular gamma camera (Sopha Medical Vision, France) equipped with ultra-high-resolution fan beam collimators and using a dose of 555 MBq of ^{99m}Tc-ethyl cysteinate dimer as CBF tracer. Details about the acquisition and preprocessing image parameters can be found elsewhere (Melie-García et al., 2013). SPECT imaging, neurological/psychiatric and neuropsychological examinations were all carried out

within a maximum interval of one month. The dataset is available at http://dx.doi.org/10.17632/3hkfsrsy6w.1

For control and MCI groups, a CBF correlation (CBF_{corr}) network was constructed as a CBF association matrix as previously described (Melie-García et al., 2013). In short, 90 brain regions of interest (ROIs) were defined as network nodes using the AAL atlas (Tzourio-Mazoyer et al., 2002). A linear regression was performed at every ROI to remove the effects of age, gender, age-gender interaction, and global values. Education level was not considered since no significant effect was shown in this parameter. Then, the Pearson's correlation coefficients across subjects between all possible pairs of ROIs were calculated (network edges) and gathered in the interregional correlation matrix (Fig.1).

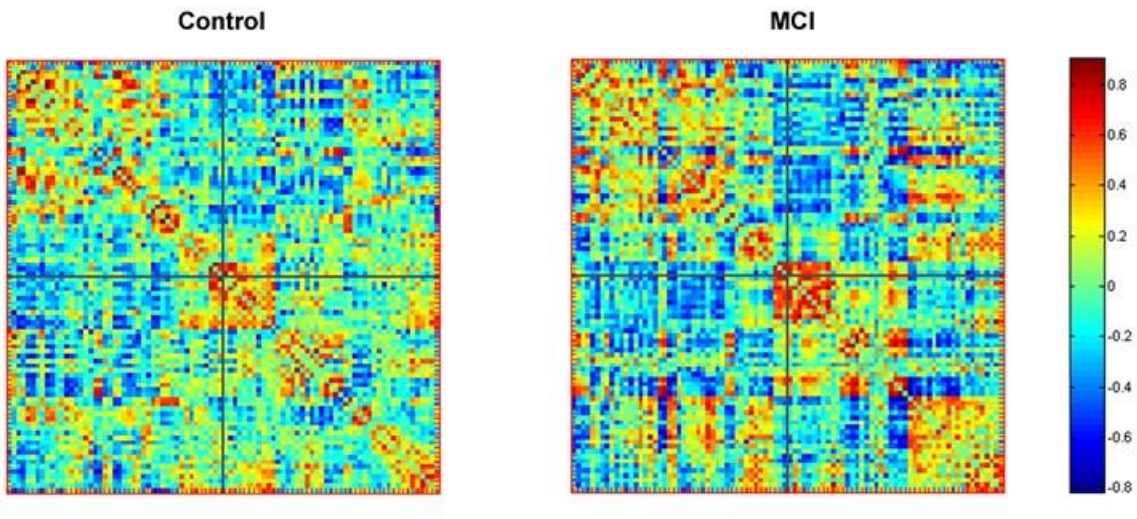

Fig. 1. CBF association matrices constructed using CBF SPECT data for control and MCI groups. The color bar indicates the value of the Pearson's correlation coefficient coming from the CBF co-variations across subjects among 90 anatomical brain regions (AAL atlas).

For the analysis, we excluded negative and self-correlations. Negative correlations were excluded since the approach used here to extract individual patient information (see subsection 2.6) was developed taking into account only positive correlations (Saggar et al., 2015).

For each CBF association matrix, binary adjacency matrices at different thresholds were then constructed (binary undirected graphs) to calculate networks topological metrics. The binary graph methodology was used as it is computationally simpler and it provides for straightforward interpretation (Rubinov and Sporns, 2010). To construct the binary graphs, the correlation coefficient was set to one (connection) if it was above a threshold and zero (no connection) otherwise. Since there is no single way to select the optimal threshold, we adopted one of the most used methods for thresholding the association matrix (De Vico Fallani et al., 2014, for a review). This method threshold the association matrix over a range of network densities and use the area under the curve (AUC) across the threshold range as a descriptor of a given network metric. A network density represents the proportion of supra-threshold connections of all possible connections. To be confident that we were analyzing the data in a safe non-random (non-regular) range, a range of densities from 0.2 to 0.35, in steps of 0.01, was used (based on preliminary explorations of the data). Previous observations have found that when the density is too high or too low, the brain graph cannot be differentiated from a random or regular network, respectively (Achard and Bullmore, 2007).

2.4. Network metrics

In the following paragraphs, we define the global network metrics used in this study.

The global network modularity reflects the extent to which a network can be subdivided into modules (communities of nodes) with a maximal within-module and minimal between-module connectivity. For the modularity analysis, we used the method developed by Newman

(Newman, 2004) to compare our results with previous studies that used this method in other neuroimaging modalities (Buldú et al., 2011; Brier et al., 2014; Catricalà et al., 2015; Daianu et al., 2014; de Haan et al., 2012; Pereira et al., 2016; Sun et al., 2014; Wang et al., 2013). The global modularity (Q) can be expressed as:

$$Q = \sum_{k \in M} [c_{kk} - (\sum_{l \in M} c_{kl})^2] \quad (1)$$

where *k* and *l* are individual modules in the set of modules M, and *c* is the proportion of existing connections between 2 modules.

We also explored the modular structure in each CBF_{corr} network (control and MCI). The community of modules with highest maximized modularity value across all possible partitions was used as representative of the modular structure of each network. We used 1000 iterations to optimize modular structures quantification as implemented in the GAT toolbox (Hosseini et al., 2012).

On the other hand, the global efficiency is a metric of network integration and reflects how efficiently the information can be exchanged over the network, considering a parallel system in which each node sends information concurrently along the network (i.e. how well connected are any pair of nodes) (Rubinov and Sporns, 2010). The global efficiency (E_{glob}) for a binary and undirected graph *G* is calculated as:

$$E_{glob}(G) = \frac{1}{N(N-1)} \sum_{\substack{i,j \in G \\ i \neq j}} \frac{1}{d_{ij}} \quad (2)$$

where *N* represents the number of nodes and d_{ij} is the shortest path length between node *i* and node *j* in *G*. The shortest path length (distance) is the minimum number of edges between node *i* and *j*.

Lastly, the local efficiency is a metric of network segregation and reflects the efficiency of the communication among the neighbors of each particular node (i.e. how well neighbors of a

node are connected) (Rubinov and Sporns, 2010). The mean local efficiency is thus the average of local efficiency across all nodes in the network. The mean local efficiency (E_{loc}) for a binary and undirected graph G is calculated as:

$$E_{loc}(G) = \frac{1}{N}\sum_{i \in G} E_{loc}, i \quad (3)$$

where E_{loc},i, is the local efficiency for a node i and is defined as:

$$E_{loc}, i = \frac{\sum_{\substack{j,h \in G \\ j \neq i}} a_{ij}\, a_{ih} \left[d_{ij}(G_i)\right]^{-1}}{k_i\,(k_i - 1)} \quad (4)$$

where a_{ij} is the connection status between i and j: a_{ij} = 1 when link (i, j) exists (when i and j are neighbors); a_{ij} = 0 otherwise (a_{ii} = 0 for all i). k_i is the degree of node i (number of links connected to node i).

We also analyzed the characteristic path length, inversely related to E_{glob}, which topologically reflects the measure of the typical separation between two nodes; the clustering coefficient, directly related to E_{loc}, that reflects the inherent tendency to cluster nodes into strictly connected neighborhoods; and the small-worldness index which is a measure to what extent a network shows an optimal balance between segregation and integration. The detailed mathematical description of these network metrics can be found elsewhere (Rubinov and Sporns, 2010).

The descriptors used for network metrics defined above, were: the AUC extracted from thresholding across the range of network densities described above and the metrics at the minimum density of 0.2.

2.5. Network metrics comparison

For testing the differences between networks (control and MCI) for each metric in every density, a nonparametric permutation t-test was used (1000 permutations). The permutation procedure was carried out using the GAT toolbox (Hosseini et al., 2012). This procedure

follows 6 steps: 1) during each permutation, ROIs data of each subject are randomly reassigned to one of the two groups so that each randomized group has the same number of participants as the original ones; 2) the association matrix is calculated for each randomized group; 3) binary adjacency matrices at different densities are obtained by applying thresholds (in the range described in the subsection 2.3); 4) network metrics are estimated for all random networks in each density; 5) differences in network metrics between randomized groups, in each density, are obtained resulting in a permutation distribution of the difference under the null hypothesis; 6) the real difference between groups in network metrics (for each density) is placed in the corresponding permutation distribution and a p-value of two tails is calculated based on its percentile position. As critical values, the 95% confidence intervals (CI) of each network metric distribution were considered (two-tailed test of the null hypothesis at $p < 0.05$).

The metrics that showed significant differences in the MCI group network as compared to the control were then used for the individual patient contribution analysis.

2.6. Individual patient contribution to network metrics and its relation to the episodic memory of MCI patients

The methodology utilized to extract the individual contribution of each MCI patient was one of the approaches proposed by Saggar et al. (2015). This methodology is based on the add-one-patient (AOP) approach and global network metrics. The AOP was adopted since it has the advantage that can be used in clinical practice, in contrast to the other method proposed by the authors based on the "leave-one-out" (LOO) approach.

The AOP approach is defined as follows: the individual contribution of a given patient, to a given metric, is estimated by subtracting the metric of the network constructed using control subjects only from the metric using control subjects plus the patient. The patient contribution to a given metric is calculated as:

$$Patient\ contribution\ = Metric\ (controls\ +\ patient) - Metric\ (controls)$$

The AUC value of each metric was used for the individual patient contribution estimation to avoid a dependency on a particular network density.

To evaluate the association between the episodic memory (RCFT) and the individual patient contribution to a specific network metric, we used the non-parametric Kendall Tau rank correlation, which is more appropriate for small samples and much less sensitive to outliers compared with Spearman's correlation (Kendall, 1962). For significant p-values, we computed 95% percentile bootstrap CIs.

In addition, we assessed the association between the episodic memory and the composite ROI index, which is a classical measure previously proposed for FDG-PET analysis in AD patients (Jagust et al., 2010) and compared effect sizes found by the two methodologies. This analysis allowed us to compare the connectivity-based approach proposed in this study and the well-established methodology based on the composite ROI index. To enable this analysis, we first generated 1000 bootstrap samples of the two datasets and the corresponding tau coefficients. Then, the Pearson correlation coefficients were derived from the computed tau coefficients, with which Fisher's z transformations were calculated (Walker, 2003). To assess the effect size differences between the two methodologies, we computed the distribution of the difference of both bootstrap samples (absolute values of Fisher's z) and the corresponding 95% percentile CI. A significant difference was considered if the CI did not contain the real observed difference.

As a supplementary analysis, we investigated whether the association found between the episodic memory and the individual subject contribution to the global network modularity (see results) was present for the control subjects as well using the LOO approach (Saggar et

al., 2015). We also explored the association between the individual contribution to network metrics and the MMSE at baseline and one-year follow-up.

The association between the episodic memory and the individual patient contribution to a specific network metric (or the composite ROI index) and differences between groups in demographic and cognitive variables were analyzed using STATISTICA software (Stat Soft, Inc, version 8.0). The significance level was set at a p-value < 0.05.

3. Results

As shown in Table 1, episodic memory (RCFT delayed recall) and MMSE were significantly reduced in the MCI group as compared to the control group. As expected, other cognitive variables showed no significant differences between groups as only MCI patients with memory complaints as the main cognitive symptom were included. Three out of twenty-four MCI patients progressed to dementia, according to NINDS/ADRDA criteria for probable AD.

On the other hand, network metric comparisons showed that the global modularity increased while the global efficiency/characteristic path length decreased/increased in the MCI group network as compared to the control (Figs. 2.a-2.c, Table 2). In contrast, the mean local efficiency, the clustering coefficient and the small-worldness index showed no significant difference (Figs. 2.d-2.f, Table 2).

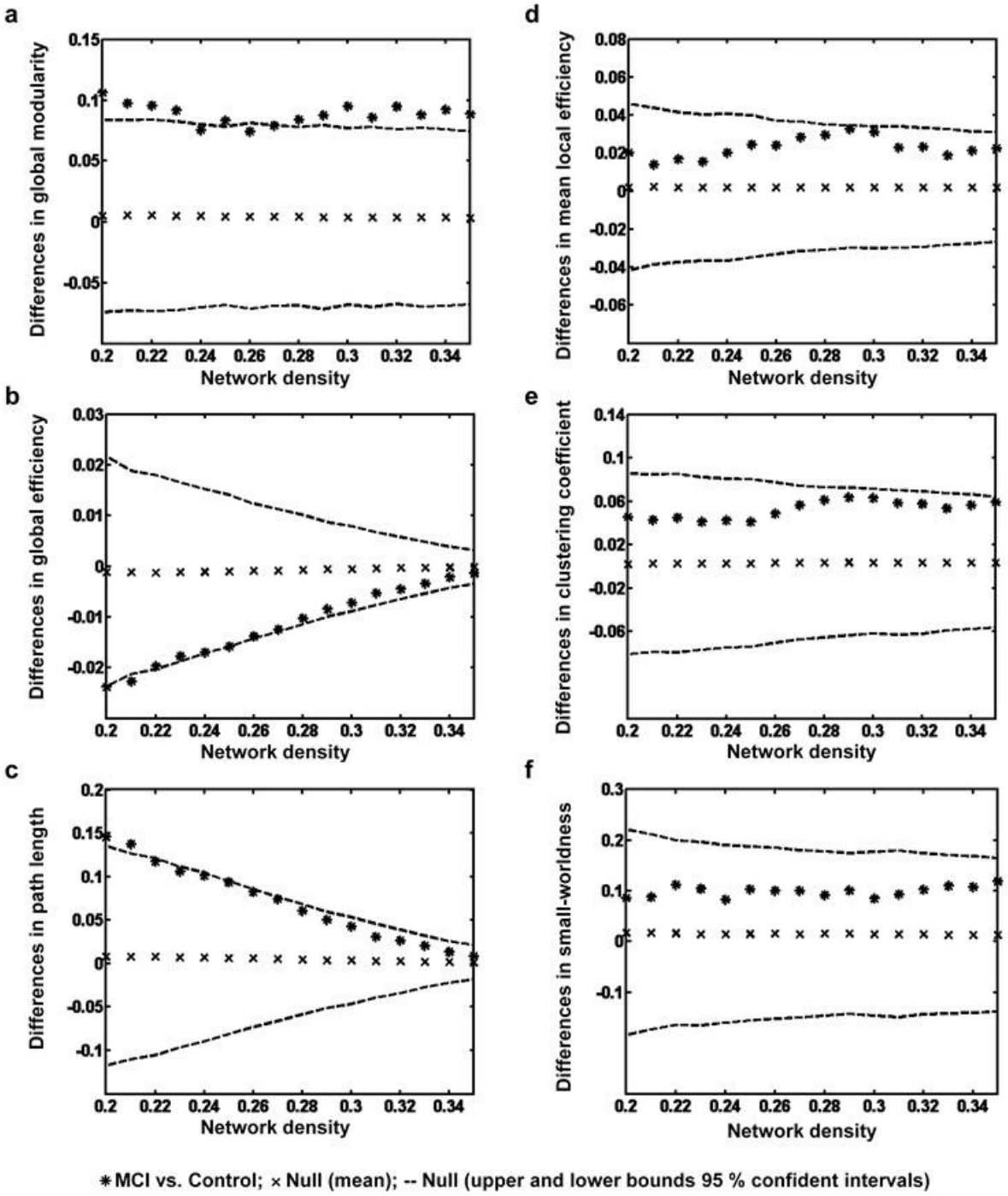

Fig. 2. Differences in network metrics (global modularity, global efficiency, path length, mean local efficiency, clustering coefficient and small-worldness) when comparing the MCI group network with the control across a range of network densities. The comparison was performed using a nonparametric permutation t-test (1000 permutations) giving expected mean effects as well as 95% confidence intervals of the null hypothesis.

Table 2 Network metrics comparison. MCI versus Control.

	Control	MCI	p-value	Percentage of change
Global modularity (AUC)	3.82E-02	5.13E-02	0.02*	+35
Global modularity (Min)	2.89E-01	3.96E-01	0.02*	+37
Global efficiency (AUC)	9.40E-02	9.22E-02	0.066	-1.9
Global efficiency (Min)	5.75E-01	5.52E-01	0.04*	-4
Path length (AUC)	2.63E-01	2.74E-01	0.066	+4.2
Path length (Min)	1.93	2.07	0.03*	+7.3
Mean local efficiency (AUC)	10.94E-02	11.41E-02	0.12	+4.3
Mean local efficiency (Min)	7.14E-01	7.54E-01	0.1	+5.6
Clustering coefficient (AUC)	7.16E-2	8.08E-02	0.30	+12.8
Clustering coefficient (Min)	4.72E-01	5.46E-01	0.25	+15.7
Small-worldness (AUC)	2.62E-1	2.73E-1	0.59	+4.2
Small-worldness (Min)	2.03	2.11	0.65	+3.9

AUC, area under curve across network density range; Min, minimum network density.

*Significant difference.

Based on the above findings, we used the global modularity and global efficiency for the individual patient contribution analysis. We found a significant negative correlation between the episodic memory and the individual patient contribution to the global modularity (Kendall Tau = -0.32; p= 0.02; CI: -0.69, -0.016) (Fig. 3.a). Unlike the global modularity, the global efficiency showed no correlation (Kendall Tau = -0.03; p= 0.81) (Fig. 3.b).

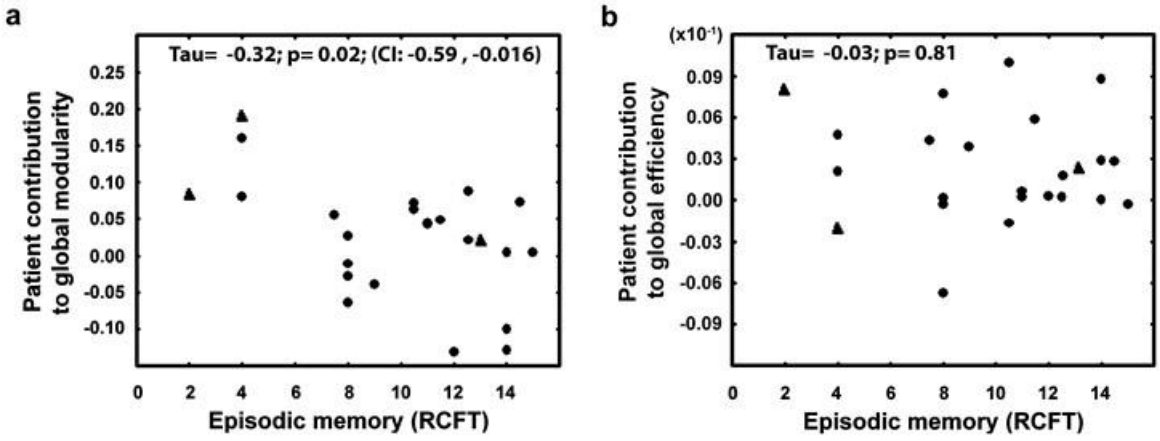

Fig. 3. Scatter plots of episodic memory scores of MCI patients and their individual contribution to the global network modularity (a) and to the global efficiency (b). The episodic memory shows a negative correlation with the patient contribution to the global network modularity (a). The three patients that progressed to probable AD dementia are plotted by triangles.

We also observed that two out of three patients that progressed to probable AD dementia had some of the lowest values of episodic memory (RCFT score of 2 and 4, respectively) and also some of the highest values of individual contributions to the global modularity (0.08 and 0.19 respectively) (Fig. 3.a). The third patient had a relatively high value of episodic memory compared with other MCI patients (RCFT score= 13) and an individual contribution to the global modularity of 0.02.

At the same time, we found a significant positive correlation between the episodic memory and the composite ROI index (Kendall Tau = 0.31; p= 0.03; CI: 0.58, 0.043) (Fig. 4). Moreover, there were no significant differences in effect sizes using the composite ROI index and the individual patient contribution to the global modularity (observed difference for Fisher's z= 0.027; CI for the bootstrap distribution: -0.028, 0.029).

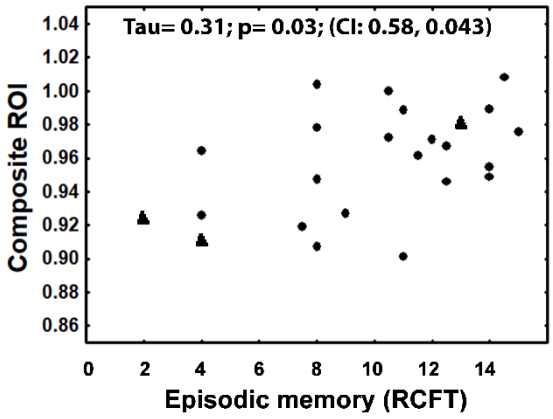

Fig. 4. Scatter plot of episodic memory scores of MCI patients and the composite ROI index. The three patients that progressed to probable AD dementia are plotted by triangles.

The supplementary analysis showed no significant association between the episodic memory and the individual subject contribution to the global network modularity for control subjects using the LOO approach (Kendall Tau = -0.15; p= 0.27, Supplementary fig. S1). There was also no correlation between the MMSE and the individual patient contribution to the global modularity neither to the global efficiency, both at baseline and one-year follow-up (Supplementary Table S1).

Modular structures:

Five modules were identified in the control group network (Fig. 5, Supplementary Table S2). Although there were no perfect matches with known large-scale functional brain networks (Menon, 2015), control module I (22 ROIs) appears to represent visual networks since it comprised areas of the occipital lobe, inferior temporal, temporoparietal and limbic regions that are known to be part or strongly connected with visual pathways. This module also included lateral prefrontal regions associated with attentional networks. Control module IV (11 ROIs) resembled sensorimotor networks, mainly comprising the post and precentral

regions bilaterally. This module also included lateral prefrontal and occipital regions on the right side. Control module V (27 ROIs) included hippocampus and lateral temporal cortex bilaterally and left temporoparietal and medial prefrontal cortices and right precuneus, which seems to resemble a part of the default mode network (DMN). This module also included both amygdala and superior parietal and occipital regions of both hemispheres, and Wernicke's area (part of language network). Control module II (15 ROIs) resembled another part of the DMN, mostly including medial prefrontal. This module also comprised angular, supramarginal and parahippocampal gyri on the right side, which are part of the DMN as well. Control module III (15 ROIs) seems to represent another part of the DMN since it comprised the cingulate cortex, including the posterior cingulate bilaterally, and other medial prefrontal areas and inferior parietal cortex on the left side, including Broca's area (part of language network). This module also included the thalamus and caudate bilaterally and primary auditory cortex on the left side.

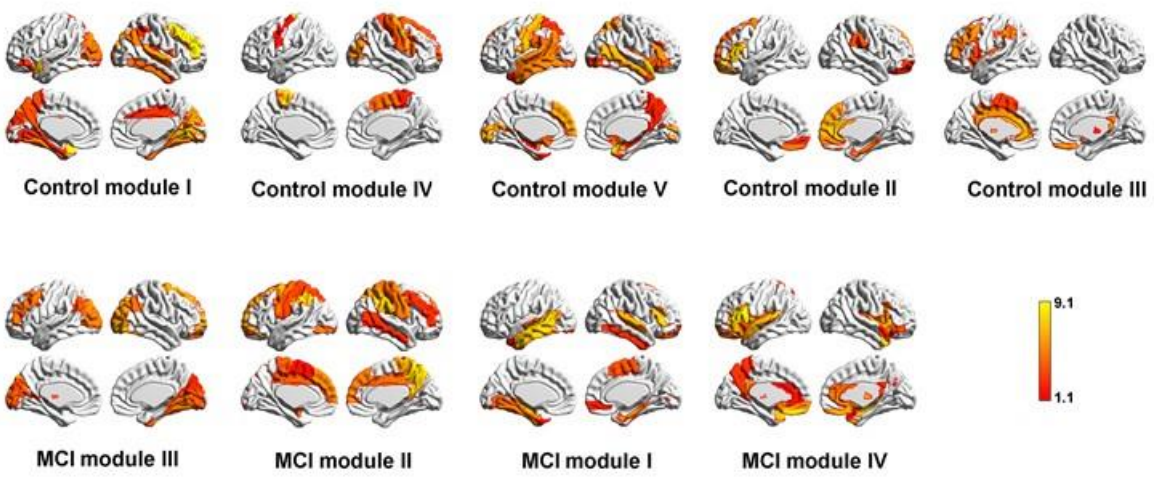

Fig. 5. Modules identified in the control and MCI group-based correlation CBF networks. Modules are visualized using AUC values of nodal degree onto the cortical surfaces by the BrainNet Viewer package (http://www.nitrc.org/projects/bnv).

On the other hand, only four modules were identified in the MCI group network (Fig. 5, Supplementary Table S2). These four modules appear as reconfigurations of different parts of the five control modules. MCI module III (17 ROIs) was mostly a greater part of control module I (visual networks), but it also included small parts of control module III and IV. MCI module II (25 ROIs) was a regrouping of parts of control modules II-V, mainly seen as sensorimotor and small DMN fragments. MCI module I (16 ROIs) mainly included small parts of control modules I, II, and V (combined part of visual networks and small DMN fragments). MCI module IV (32 ROIs) was the biggest and mainly consisted of regrouping parts of control modules II, III, and V, delineating better an important part of the medial segment of the DMN as a single module.

4. Discussion

In this study, we investigated whether the episodic memory of amnestic MCI patients is associated with the individual patient contributions to topological metrics of the group-based CBF SPECT correlation network using the add-one-patient (AOP) approach. We found that the individual patient contribution to the global network modularity inversely correlates with episodic memory, which highlights the potential of this approach to develop a CBF connectivity-based biomarker at the individual level for MCI patients.

The increase in the global modularity in the MCI network suggests more abnormal organization in the patients with a higher individual contribution to this metric. This would be counterintuitive if the global modularity only depended on the number of modules (more modules might suggest more adaptability of the network in case one of the modules is damaged). However, the global modularity also depends on two other factors: within-module and between-module connectivity (subsection 2.4, equation 1). That the number of modules decreased in the MCI network, whereas the global modularity increased, could be explained

by the decrease in the between-module connectivity (consistent with a lower global efficiency, Fig. 2.b) and the increase in the within-module connectivity (see the tendency to a higher mean local efficiency in Fig. 2.d). Thus, the MCI network seems to be reconfigured in such a way that in a smaller number of less interconnected modules more nodes are regrouped.

This interpretation is in agreement with a recent study that utilized group-based correlation networks derived from sMRI (Pereira et al., 2016). The authors found that the global modularity was increased in larger groups of amnestic MCI patients (early and late onset samples) that progressed to AD dementia. Similar to our results, they also found that the number of modules decreased in MCI groups, "suggesting that their whole-brain networks were fragmented into a few large, isolated components" (Pereira et al., 2016). de Haan et al. (2012) reported comparable findings in low frequencies (delta and theta) bands using resting-state MEG data in AD patients with mild to moderate dementia. Furthermore, two other studies also showed that the global modularity increases in amnestic MCI patients, one using DTI (Daianu et al., 2014) and another by fMRI during a memory task (Catricalà et al., 2015).

Interestingly, the biggest module identified in the MCI network suggests a regrouping of brain regions that partially resembles the medial segment of the DMN (MCI module IV in Fig. 5). As discussed above, the reconfiguration of the MCI network and the increase in global modularity are related. Therefore, the patients that contributed more to the network reconfiguration were also the ones that contribute more (as a tendency) to the increase in global modularity and, in turn, those with less episodic memory (Fig. 3.a). Thus, considering the overlap of the episodic memory network and the DMN (Rugg and Vilberg, 2013) which is a target of the AD process (Villain et al., 2012), the regrouping of brain regions around the DMN might explain the negative correlation found between the episodic memory and the individual patient contribution to the global modularity. Consequently, the network reconfiguration might reflect the effects of the pathological process. This interpretation is in

line with a recent connectivity study in multiple sclerosis (MS) patients using resting-state fMRI data (Gamboa et al., 2014). The authors also observed that cognitive function in MS patients negatively correlates with the global modularity.

The lack of association between episodic memory and the individual subject contribution to the global modularity found in healthy controls is consistent with the link between the network reconfiguration (apparently related to the pathological process) and the increase in global modularity in the MCI group explained above. Alternatively, it might be due to the sample size since a trend toward a negative correlation, similar to MCI group, was also observed.

On the other hand, it would be expected that when a patient is added to the control network, the global modularity would increase in the resulting network. However, the contribution was negative in a subgroup patient (Fig. 3.a). This is probably due to two factors: 1) the sample size of control and MCI subjects. In larger samples, the proportion of patients with a negative contribution would decrease because the variability of both groups would be less. Nevertheless, the sample size of controls also has a limit (close to $n = 100$) as the absolute individual contribution tends asymptotically to zero as the sample size increases for the AOP approach (Saggar et al., 2015); and 2) the magnitude of the difference between groups for each network metric also counts. For instance, in the case of global efficiency, where the difference between groups (in the opposite direction) was less as compared with global modularity (Fig.2), the proportion of patients with a positive contribution was much higher (Fig. 3.b). However, the influence of these two factors would not change the association found between the episodic memory and the individual patient contribution to global modularity, since this only depends on the absolute value of the individual contribution using the AOP approach (Saggar et al., 2015).

We also found no association between the individual patient contribution to the global modularity (neither to the global efficiency) and MMSE at baseline and one-year follow-up (Supplementary material). These findings could be explained by the fact that the changes in MMSE are less specific than the episodic memory decline in MCI patients that progress to AD dementia. Although the MMSE is useful to verify longitudinal intra-individual changes of global cognitive function, its sensitivity is low for MCI (Tombaugh and McIntyre, 1992).

In contrast to our results, other studies have found that the global modularity decreases in patients with amnestic MCI by using fMRI (Brier et al., 2014; Sun et al., 2014; Wang, et al., 2013) and MEG (Buldú et al., 2011). Although this discrepancy may be due to methodological differences, or sample composition, it is more likely that this discrepancy reflects the different biological processes that are assessed by each modality, or even within a modality (Dai and He, 2014; Tijms et al., 2013 for reviews). To illustrate this, de Haan et al. (2012) not only found an increase in global modularity in the low frequencies (delta and theta bands), as discussed above, but also found that the global modularity decreases in the high frequencies (beta and gamma bands). The similarity with our results in the low frequencies and the opposite in the high frequencies bands could be explained by the correlation previously observed between the CBF and the low frequencies of the cerebral electrical activity, but not with the high frequencies (Menon et al., 1980). Similarly, two earlier reviews have suggested that diverging findings across neuroimaging modalities are because different modalities measure different aspects of brain connectivity (Dai and He, 2014; Tijms et al., 2013). Even more, a recent study has shown that the change in the brain network topology could be non-monotonic as the AD progresses (Kim et al., 2015), implying that the network topology could show even opposite results between two different time-points.

Whereas global modularity increased, we also observed that network integration was decreased in the MCI network, as indicated by the reduction in the global efficiency. This is

consistent with the majority of literature where different neuroimaging modalities have consistently found a decrease in network integration in MCI (Dai and He, 2014; Tijms et al., 2013 for reviews), which has been interpreted as a result of brain connectivity loss. Unlike the global modularity, we found no significant correlation between the episodic memory and the global efficiency. Perhaps the global efficiency is more associated with the global cognitive function in more advanced stages of the disease, which is in line with previous studies that found a negative correlation between the characteristic path length, inversely related to the global efficiency, and the MMSE in patients with AD dementia (Dai and He, 2014; Tijms et al., 2013 for reviews).

Lastly, it was observed that the effect size of the connectivity-based metric proposed in this study was comparable to the metric based on the composite ROI index (Jagust et al., 2010). However, to determine whether the global modularity is a good predictor of progression to AD dementia in MCI patients, longitudinal studies (with 2 or more years follow-up) in larger patient samples are required and outcomes should be compared with classical predictors of AD dementia. In this sense, the present investigation could be considered a pilot study that needs further validation.

This study has limitations. First, the methodology applied for extracting the individual patient contribution was based on global network metrics. It is possible that a methodology based on network metrics at the regional level (yet to be validated) could capture a stronger relationship with episodic memory in MCI patients since the network for the episodic memory involves specific brain regions (Rugg and Vilberg, 2013). Second, although our patients fulfilled clinical criteria for MCI due to AD, some of the suggested explanations need further validation in MCI patients with confirmed AD pathology. Finally, graph theoretical analysis of the CBF correlation network has limitations that were discussed in our previous article (e.g. the use of Pearson's correlation instead of partial correlation; choice of parcellation scheme;

possible variability of results with different sample sizes) (Melie-García et al., 2013). Nevertheless, the effects of these limitations on the individual-level analysis may be small. For example, Saggar et al. (2015) found that the absolute individual contribution to global network metrics stabilizes around *n*=25-30 (for the control group) using the AOP approach.

In conclusion, our findings suggest that episodic memory in MCI patients inversely correlates with the patient contribution to the global modularity of the CBF network, which warrants further research to develop a CBF connectivity-based biomarker at the individual level. Furthermore, this study confirms previous findings by other neuroimaging modalities that brain connectivity is altered in MCI.

Acknowledgements

The authors thank the collaboration of Drs. Yurelis Ginarte and David Vállez García and the support of the Center for Neurological Restoration (CIREN), Havana, Cuba, the Department of Nuclear Medicine and Molecular Imaging, and the Department of Neurology and Alzheimer Research Center, University Medical Center Groningen, the Netherlands.

Contributors

CASC, AW, PPD, YIM, and LMG developed the study concept with input from RB, RD, and PPD. Clinical and neuropsychological evaluations were performed by JSN with assistance from AAR and PPD. SPECT data was acquired by AAR with assistance from CASC. CASC, YIM, and LMG performed statistical analyses and interpreted the data under the supervision of AW, RB, RD, and PPD. CASC wrote the manuscript, and AW, RB, PPD, RD, YIM, and LMG provided critical revisions.

Conflicts of Interest

All authors declared that they have no conflict of interest relevant to the subject matter of the manuscript.

References:

Achard, S., Bullmore, E., 2007. Efficiency and cost of economical brain functional networks. PLoS Comput. Biol. 3 (2), e17.

Albert, M.S., DeKosky, S.T., Dickson, D., Dubois, B., Feldman, H.H., Fox, N.C., et al., 2011. The diagnosis of mild cognitive impairment due to Alzheimer'sdisease: recommendations from the National Institute on Aging-Alzheimer's Association workgroups on diagnostic guidelines for Alzheimer's disease. Alzheimers Dement. 7, 270–279.

Batalle, D., Muñoz-Moreno, E., Figueras, F., Bargallo, N., Eixarch, E., Gratacos, E., 2013. Normalization of similarity-based individual brain networks from gray matter MRI and its association with neurodevelopment in infants with intrauterine growth restriction. NeuroImage. 83, 901–911.

Brier, M.R., Thomas, J.B., Fagan, A.M., Hassenstab, J., Holtzman, D.M., Benzinger, T.L., et al., 2014. Functional connectivity and graph theory in preclinical Alzheimer's disease. Neurobiol.Aging. 35, 757–768.

Buldú, J.M., Bajo, R., Maestú, F., Castellanos, N., Leyva, I., Gil, P., et al., 2011. Reorganization of functional networks in mild cognitive impairment. PLoS One, 6 (5), e19584.

Catricalà, E., Della Rosa, P.A., Parisi, L., Zippo, A.G., Borsa, V.M., Iadanza, A., et al., 2015. Functional correlates of preserved naming performance in amnestic Mild Cognitive Impairment. Neuropsychologia. 76,136-152.

Daianu, M., Jahanshad, N., Nir, T.M., Leonardo, C.D., Jack, C.R. Jr, Weiner, M.W., et al. ,2014. Algebraic connectivity of brain networks shows patterns of segregation leading to reduced network robustness in Alzheimer's disease. Comput Diffus MRI. 2014, 55–64. doi: 10.1007/978-3-319-11182-7_6

Dai, Z., He, Y., 2014. Disrupted structural and functional brain connectomes in mild cognitive impairment and Alzheimer's disease. Neurosci Bull. 30, 217–232.

de Haan, W., vanderFlier, W.M., Koene, T., Smits, L.L., Scheltens, P., Stam, C.J., 2012. Disrupted modular brain dynamics reflect cognitive dysfunction in Alzheimer's disease. NeuroImage. 59, 3085–3093.

De Vico Fallani, F., Richiardi, J., Chavez, M., Achard, S., 2014. Graph analysis of functional brain networks: practical issues in translational neuroscience. Philos Trans R Soc Lond B Biol Sci. 369(1653). pii: 20130521. doi: 10.1098/rstb.2013.0521.

Folstein, M.F., Folstein, S.E., McHugh, P.R.,1975. "Mini-mental status". A practical method for grading the cognitive state of patients for the clinician. Journal of Psychiatric Research. 12, 189–198.

Fornito, A., & Bullmore, E.T. ,2015. Connectomics: a new paradigm for understanding brain disease. Eur Neuropsychopharmacol. 25, 733-748.

Gamboa, O.L, Tagliazucchi, E., von Wegner, F., Jurcoane, A., Wahl, M., Laufs, H., et al., 2014. Working memory performance of early MS patients correlates inversely with modularity increases in resting state functional connectivity networks. NeuroImage. 94, 385-395.

Hamilton, M., 1960. A rating scale for depression. J Neurol Neurosurg Psychiatry. 23, 56-62.

Hosseini, S.M.H., Hoeft, F., Kesler, S.R., 2012. GAT: A Graph-Theoretical Analysis Toolbox for Analyzing Between-Group Differences in Large-Scale Structural and Functional Brain Networks. PLoS One. 7 (7), e40709.

Jagust,W.J., Bandy, D., Chen, K., Foster, N.L., Landau, S.M., Mathis, C.A., et al., 2010. The Alzheimer's Disease Neuroimaging Initiative positron emission tomography core. Alzheimers Dement. 6, 221-229.

Jie, B., Zhang, D., Wee, C. Y., Shen, D., 2014. Topological graph kernel on multiple thresholded functional connectivity networks for mild cognitive impairment classification. Human Brain Mapping. 35, 2876–2897.

Kendall, M.G., 1962. Rank Correlation Methods, third ed. Hafner Publishing Company, New York.

Kim, H., Yoo, K., Na, D.L., Seo, S.W., Jeong, J., Jeong, Y., 2015. Non-monotonic reorganization of brain networks with Alzheimer's disease progression. Front Aging Neurosci. 9;7: 111. doi: 10.3389/fnagi.2015.00111. eCollection 2015.

Lezak, M.D.,1983. Neuropsychological assessment, second ed. Oxford University Press, New York.

Liang, X., Tournier, J.D., Masterton, R., Connelly, A., Calamante, F., 2012. A k-space sharing 3D GRASE pseudocontinuous ASL method for whole-brain resting-state functional connectivity. Int. J. Imaging Syst. Technol. 22, 37–43.

Liang, X., Zou, Q., He, Y., Yang Y., 2013. Coupling of functional connectivity and regional cerebral blood flow reveals a physiological basis for network hubs of the human brain. Proc Natl Acad Sci U S A. 110, 1929-1934.

Liang, X., Connelly, A., Calamante, F., 2014. Graph analysis of resting-state ASL perfusion MRI data: nonlinear correlations among CBF and network metrics. Neuroimage. 87, 265-275.

Melie-García, L., Sanabria-Diaz, G., Sánchez-Catasús, C., 2013. Studying the topological organization of the cerebral blood flow fluctuations in resting state. NeuroImage 64. 173–184.

McKhann, G., Drachman, D., Folstein, M., Katzman, R., Price, D., Stadlan, E.M., 1984. Clinical diagnosis of Alzheimer's disease Report of the NINCDS−ADRDA WorkGroup* under the auspices of department of health and human services task force on Alzheimer'sdisease. Neurology. 34, 939–939.

Menon V.,2015. Large-Scale Functional Brain Organization. In: Arthur W. Toga, editor. Brain Mapping: An Encyclopedic Reference, vol. 2, pp. 449-459. Academic Press: Elsevier.

Menon, D., Koles, Z., Dobbs, A., 1980. The relationship between cerebral blood flow and the EEG in normals. Can J Neurol Sci. 3, 195-198.

Mondini, S., Mapelli, D., Vestri, A., 2005. Esame neuropsicologico breve. Raffaello Cortina Editore, Milan.

Morris, J.C., 1993. The clinical dementia rating (CDR): current version and scoring rules. Neurology. 43, 2412–2414.

Newman, M.E.J., 2004. Fast algorithm for detecting community structure in networks. Phys Rev E Stat Nonlin Soft Matter Phys. E 69, 066133.

Pereira, B., Mijalkov, M., Kakaei, E., Mecocci, P., Vellas, B., Tsolaki, et al., 2016. Disrupted Network Topology in Patients with Stable and Progressive Mild Cognitive Impairment and Alzheimer's Disease. Cereb Cortex. 26, 3476-3493.

Quaranta, D., Gainotti, G., Di Giuda, D., Vita, M., G., Cocciolillo, F., Lacidogna, G., et al., 2018. Predicting progression of amnesic MCI: The integration of episodic memory impairment with perfusion SPECT. Psychiatry Res Neuroimaging. 271, 43-49.

Raj, A., Mueller, S.G., Young, K., Laxer, K.D., Weiner, M., 2010. Network-level analysis of cortical thickness of the epileptic brain. NeuroImage. 52, 1302–1313.

Ramanan, S., Flanagan, E., Leyton, C.E., Villemagne, V.L., Rowe, C.C., Hodges, et al., 2016. Non-Verbal Episodic Memory Deficits in Primary Progressive Aphasias are Highly Predictive of Underlying Amyloid Pathology. J Alzheimers Dis. 51, 367-76.

Rubinov, M., Sporns, O., 2010. Complex network measures of brain connectivity: uses and interpretations. NeuroImage. 52, 1059–1069.

Rugg, M.D., Vilberg, K.L., 2013. Brain networks underlying episodic memory retrieval. Curr. Opin. Neurobiol. 23, 255–260.

Saggar, M., Hosseini, S.M., Bruno, J.L., Quintin, E.M., Raman, M.M., Kesler, et al., 2015. Estimating individual contribution from group-based structural correlation networks. NeuroImage. 120, 274–284.

Sanabria-Diaz, G., Martinez-Montes, E., Melie-Garcia, L., 2013. Glucose metabolism during resting state reveals abnormal brain networks organization in the Alzheimer's disease and mild cognitive impairment. PLoS One. 8 (7), e68860.

Sánchez-Catasús, C.A., Stormezand, G.N., van Laar, P.J., De Deyn, P.P., Sánchez, M.A., Dierckx, R.A., 2017. FDG-PET for prediction of AD dementia in mild cognitive impairment. A review of the state of the art with particular emphasis on the comparison with other neuroimaging modalities (MRI and perfusion SPECT). Curr. Alzheimer Res. 14, 127–142.

Sánchez-Catasús, C.A., Sanabria-Diaz, G., Willemsen, A., Martinez-Montes, E., Samper-Noa, J., Aguila-Ruiz, A., et al., 2017. Subtle alterations in cerebrovascular reactivity in mild

cognitive impairment detected by graph theoretical analysis and not by the standard approach. Neuroimage Clin. 15, 151-160.

Sánchez Catasús, Carlos Alfredo (2018), "CBF SPECT and demographic/cognitive data of MCI patients and healthy controls.", Mendeley Data, v1

http://dx.doi.org/10.17632/3hkfsrsy6w.1

Seo, E.H., Lee, D.Y., Lee J.M., Park J.S., Sohn B.K., Lee D.S., et al., 2013. Whole-brain functional networks in cognitively normal, mild cognitive impairment, and Alzheimer's disease. PLoS One. 8(1), e53922.

Son, S.J., Kim, J., Seo, J., Lee, J.M., Park, H.; ADNI, 2015. Connectivity analysis of normal and mild cognitive impairment patients based on FDG and PiB-PET images. Neurosci Res. 98, 50-58.

Spinnler, H., Tognoni, G., 1987. Italian standardization and classification of neuropsychological tests. Ital J Neurol Sci. 6 (Suppl 8), 1–120, 1987.

Sun, Y., Yin, Q., Fang, R., Yan, X., Wang, Y., Bezerianos, A., Sun, J., 2014. Disrupted functional brain connectivity and its association to structural connectivity in amnestic mild cognitive impairment and Alzheimer's disease. PLoSOne. 9(5), e96505.

Tijms, B.M., Seriès, P., Willshaw, D.J., Lawrie, S.M., 2012. Similarity-based extraction of individual networks from gray matter MRI scans. Cereb. Cortex. 22, 1530–1541.

Tijms, B.M., Wink, A.M., de Haan, W., van der Flier, W.M., Stam, C.J., Scheltens, P., et al, 2013. Alzheimer's disease: connecting findings from graph theoretic studies of brain networks. Neuorobiol. Aging. 34, 2023–2036.

Tombaugh, T.N., McIntyre, N.J., 1992. The mini-mental state examination: a comprehensive review. J Am Geriatr Soc. 40, 922-935.

Tzourio-Mazoyer, N., Landeau, B., Papathanassiou, D., Crivello, F., Etard, O., Delcroix, N., et al. Automated anatomical labeling of activations in SPM using a macroscopic anatomical parcellation of the MNI MRI single-subject brain. NeuroImage. 15, 273–289.

Villain, N., Chételat, G., Grassiot, B., Bourgeat, P., Jones, G., Ellis, K.A., et al., 2012. Regional dynamics of amyloid-β deposition in healthy elderly, mild cognitive impairment and Alzheimer's disease: a voxelwise PiB-PET longitudinal study. Brain. 135 (Pt 7), 2126–2139.

Viviani, R., Messina, I., Walter, M., 2011. Resting state functional connectivity in perfusion imaging: correlation maps with BOLD connectivity and resting state perfusion. PLoS One. 6(11), e27050.

Walker, D.A, 2003. JMASM9: converting Kendall's tau for correlational or meta-analytic analyses. J Mod Appl Stat Meth. 2, 525–530.

Wang, J., Zuo, X., Dai, Z., Xia, M., Zhao, Z., Zhao, X., et al., 2013. Disrupted functional brain connectome in individuals at risk for Alzheimer's disease. Biol.Psychiatry. 73, 472–481.

Zhou, L., Wang, Y., Li, Y., Yap, P.T., Shen, D., Alzheimer's Disease Neuroimaging Initiative (ADNI), 2011. Hierarchical anatomical brain networks for MCI prediction: revisiting volumetric measures. PLoS One. 6(7), e21935.